

Metal–Organic Frameworks: Why Make Them Small?

Jiemin Wang, Inhar Imaz,* and Daniel Maspoch*

Recent studies have demonstrated that metal–organic frameworks (MOFs) can be miniaturized down to the submicroscale and even nanoscale to create small MOFs. Herein, the basic concepts and recent progresses concerning the core question of “MOFs, why make them small?” are briefly introduced from three perspectives: those of size, shape, and processability. Small sizes endow MOFs with large outer surface area/volume ratios, leading to important differences in their characteristics (e.g., outer surface energy, number of defects, etc.) relative to their bulk scale counterparts and thus, opening the door to size-dependent properties such as flexibility or catalytic performance. Downsizing MOFs also enables shaping of them into unusual shapes. Among the most appealing morphologies are 2D nanosheets, whose structure can favor certain porosity-related applications. The controlled miniaturization of MOF particles also favors their integration onto surfaces and into devices as well as their colloidal stability, which in turn translates to the ability to use readily processable MOF-based liquids in countless processes, such as to drive the assembly of sophisticated meso- and macroscopic architectures, gels, monoliths, and porous liquids. It is believed that ongoing research to shrink MOFs via nanotechnology, as has been done with other classes of materials, will continue to yield novel MOF-related materials that exhibit unprecedented structural and functional properties.

pore size, shape, and functionality; and diverse structures and compositions.^[1–3] Moreover, as hosts, MOFs can selectively adsorb and release guest molecules within their cavities; boast other functionalities such as conductivity, magnetism, and optics; and exhibit unprecedented behaviors such as gate opening and flexible structural transformations. Accordingly, MOFs offer great potential for myriad applications, including removal/storage of pollutants and/or hazardous gases (e.g., CO and CO₂), fuel applications (e.g., with H₂ or CH₄), catalysis, sensing, and biomedical applications.^[4–11]

Importantly, more than 20 000 MOFs have been reported to date.^[12] However, despite their practical and industrial promise, they do not always fulfill all the requirements for their intended use. This is often down to the form in which they are synthesized: micrometer-sized crystalline powders. Indeed, for many uses, MOFs would instead have to be shaped into meso- or macroscale objects (e.g., monoliths, pellets, or membranes) or integrated into/onto polymers, surfaces, and devices.

For many other applications, MOFs must be miniaturized to the submicro- or nanoscale, such that the resulting MOF particles could be used directly as a colloidal dispersion (e.g., for biomedical applications, catalysis, etc.) or as a liquid-processable form that would facilitate integration of MOFs into/onto surfaces, devices, or membranes, combination of them with other materials to form composites, or their self-assembly. In this context, great advances have been recently made to miniaturize MOFs (hereafter called as small MOFs) down to the submicrometer regime (100–1000 nm) and even further down, to the nanoscale (≈20–100 nm), either in solution or on surfaces.^[13–21]


Research on small MOFs shows that they can exhibit size-dependent properties, similar to other nanoparticles. Moreover, researchers can now control both the size and shape of MOFs with high reproducibility and can even isolate 2D MOF nanosheets. In addition, new chemistries are expanding the scope of external surface functionalization of MOFs, as well as integration of them onto surfaces, whereby MOF growth can now be controlled down to a few nanometers. The ensemble of advances suggests that research of MOFs at this length scale is following the research pathway previously laid out for other nanomaterials (e.g., gold nanoparticles), for which control over their synthesis, homogeneity, and functionalization enables the discovery of new properties and applications. We do not intend this review to be exhaustive but rather present our concise

1. Introduction

Metal–organic frameworks (MOFs), which are built from metal ions/clusters connected through multifunctional organic linkers, are among the most attractive porous materials today, owing to their high porosity (Brunauer–Emmet–Teller surface areas up to ≈8000 m² g^{−1}); high chemical and thermal stability; tunable

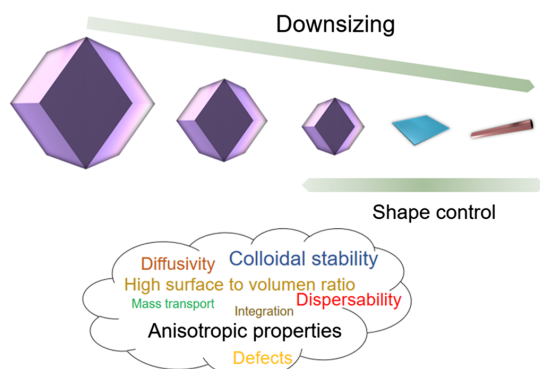
J. Wang, I. Imaz, D. Maspoch
Catalan Institute of Nanoscience and Nanotechnology (ICN2), CSIC, and
Barcelona Institute of Science and Technology
Campus UAB
Bellaterra, Barcelona 08193, Spain
E-mail: inhar.imaz@icn2.cat; daniel.maspoch@icn2.cat

D. Maspoch
ICREA
Pg. Lluís Companys 23, Barcelona 08010, Spain

 The ORCID identification number(s) for the author(s) of this article can be found under <https://doi.org/10.1002/ssstr.202100126>.

© 2021 The Authors. Small Structures published by Wiley-VCH GmbH. This is an open access article under the terms of the Creative Commons Attribution-NonCommercial-NoDerivs License, which permits use and distribution in any medium, provided the original work is properly cited, the use is non-commercial and no modifications or adaptations are made.

DOI: 10.1002/ssstr.202100126



Scheme 1. Schematic illustration of potential downsizing effects on MOFs.

vision of the unique features and advantages that controlling downsizing of MOFs can provide (Scheme 1).

2. Size

As for any other type of material, the size of MOF particles is inversely related to their surface area/volume ratio, which in turn underpins differences relative to their bulk analogs. For example, the outer surface energy of small MOFs is predominant in the total energy system, unlike in larger MOFs. Also, the number of metal ions, organic linkers, and dangling bonds exposed to outer surfaces increases with decreasing particle size. Other features, such as the defect number (on the outer surface as well as within the framework), the diffusion barriers, the mass transport capacity, and the grain boundaries, can also vary with particle size. Altogether, these differences contribute to the unique functional properties of miniaturized MOFs.

One representative size-dependent property of MOFs is structural switchability, which is the reversible structural transition of an MOF upon solvent removal and adsorption, as recently reviewed by Kaskel and co-workers.^[22] Generally, the flexibility of MOFs and consequently, their switchability decreases with decreasing particle size: accordingly, small MOFs are more structurally rigid (i.e., less switchable) than their corresponding bulk MOFs (Figure 1a). This trend, first observed in pillared-type MOFs,^[23,24] has been widely observed in flexible MOFs, in which the reversible structural transitions of bulk particles are not possible in smaller particles, whose open-pore phase, upon guest removal, instead becomes stabilized. Specific examples of such behaviors are found in MIL-53, for which downsized particles do not exhibit the breathing behavior of larger ones;^[25,26] in miniaturized zeolitic imidazolate framework (ZIF-8), which shows its typical gate-opening effect at higher pressures;^[27,28] and in DUT-49, in which the negative gas expansion of bulk particles becomes restricted at particle sizes of 1 μm and smaller.^[29] Moreover, downsizing also limits the structural mobility of interpenetrated $[\text{Cu}_2(\text{bdc})_2(\text{bpy})]_n$, hence stabilizing the metastable open-dried phase and leading to a “shape-memory effect”, which is not observed in larger crystals.^[23]

Another advantage provided by the high surface area/volume ratios shown by small MOFs that directly influence their

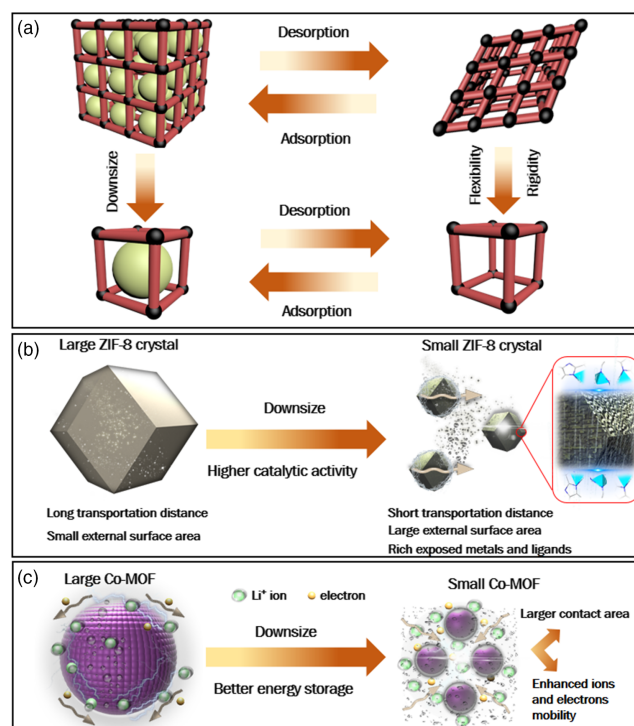


Figure 1. a) Schematic illustrating how the switchability of MOFs is dictated by particle size. b) Schematic explaining the advantages for downsized ZIF-8 crystals toward catalytic activity.^[35] c) Schematic illustration of the enhanced ion/electron transport in pulverized, ultrasmall, Co-MOF nanocrystals within a lithium-ion battery.^[37]

properties is that the number of defects and active metal ions/organic linkers exposed on their outer surfaces is higher than in the corresponding bulk MOFs. For instance, in catalysis, it can either improve their catalytic performance, increase the reaction rate, or enable catalytic reactions involving substrates larger than the pores of the MOF.^[18,30] Moreover, small MOFs can exhibit reduced diffusion barriers and improved spread of substrates and products through their pores, relative to larger MOFs.^[31,32] Researchers have recently begun to exploit these properties for catalysis. For example, Farha and co-workers studied the catalytic hydrolysis of methyl paraxon as a function of NU-1000 crystallite size, observing a significant enhancement in the hydrolysis rate for NU-1000 crystals sized 75 nm compared with crystals sized 1200 nm.^[33] Kitagawa and co-workers observed similar behavior for MOF-76(Yb), which they used to catalyze the esterification of acetic acid with methanol, finding superior catalytic performance for nanoscale crystals of MOF-76(Yb) than for microcrystals.^[34] In this particular application, etching and leaching of active substances from smaller MOF particles can also be faster than in their bulk analogs due to their larger outer surface area, thus contributing to their improved catalytic performance. This fact was confirmed by Sumbly, Doonan, and co-workers, who found that the transesterification of hexanol and vinyl acetate to produce hexyl acetate was catalyzed faster as the ZIF-8 particle size was decreased (Figure 1b).^[35]

The larger contact areas and shorter path for transportation of mass, ions, and electrons provided by small MOFs can prove

beneficial for practical and industrial applications such as energy storage.^[36] For instance, Xiao et al., working on a MOF-based anode for a lithium-ion battery, reported that pulverization of ultrasmall sub-5 nm Co-MOF particles significantly increased the contact area between this MOF and the desired electrolyte, thereby shortening the electron and ion transport pathways (Figure 1c).^[37] The authors were thus able to fabricate a battery showing excellent reversible capacity (1301 mAh g⁻¹ at 0.1 A g⁻¹), extraordinary rate performance (494 mAh g⁻¹ at 40 A g⁻¹), and outstanding cycling stability (98.6% capacity retention at 10 A g⁻¹ after 2000 cycles), all far superior to those of other reported MOF-based anodes for lithium-ion batteries.

Advantages of MOFs for chemical applications include their regularly sized pores, their polyhedral shapes, and their rich compositions based on carbon, oxygen, nitrogen, and metal ions. Combining these traits with submicrometer particle sizes affords promising templates for synthesis of metal–carbon and metal oxide particles via calcination or pyrolysis. Indeed, following this approach, myriad particles with novel compositions, shapes (an MOF's shape can be maintained during calcination/pyrolysis), and/or porosities for diverse applications have been discovered, whose synthesis would not be possible via conventional (i.e., bottom-up) routes. For example, Gascón, Marti-Gastaldo, and co-workers demonstrated that the thermal decomposition of submicrometric MUV-101(Fe, Ti) particles affords carbon-supported titanomaghemite nanoparticles.^[38] The resulting titanomaghemite showed an unprecedented Fe/Ti ratio of nearly 2:1, which cannot be achieved via soft chemistry routes. Furthermore, it exhibited outstanding performance in the catalyzing production of CO from CO₂ via the reverse water–gas shift (RWGS) reaction, with CO selectivity values of ≈100% and no signs of deactivation after several days on stream.

3. Shape

In addition to producing small 0D MOF particles by downsizing bulk crystals in all dimensions, researchers have also generated functional (magnetic, conductive, etc.),^[39–43] 2D MOF nanosheets or nanolayers, by miniaturizing MOFs while controlling their anisotropic growth or delamination. For instance, Dinca and colleagues recently prepared highly ordered Cu₃HHTT₂ nanosheets that exhibited a strong correlation between in-plane and out-of-plane conductivity.^[44] Interestingly, the two-dimensionality of MOFs can also influence their properties, including favorably for porosity-related applications. An iconic example was reported by Gascón and co-workers, who showed that Cu-BDC nanosheets of micrometer lateral dimensions and nanometer thickness could be synthesized by controlling the kinetics of MOF growth under diffusion-mediated modulation.^[45] In these nanosheets, nanopores run along the stacking direction of a few Cu-BDC layers. Incorporating MOF nanosheets into polymer matrices, positioned at nearly 90° relative to the gas flow direction, confers the resultant composites with outstanding performance at separating CO₂ from CO₂/CH₄ gas mixtures (Figure 2a). Moreover, the resultant nanosheet/matrix hybrids exhibit equal or slightly superior gas separation selectivity on increasing the upstream pressure, an opposite behavior to that observed for the neat polymeric membrane and for the

MOF–polymer membrane made with the corresponding isotropic (bulk) MOF.

Intriguingly, the aforementioned size-related benefits of small MOFs are even greater in MOF nanosheets. For instance, the surface exposure of active metal ions/linkers is much higher in 2D systems. In this sense, Tang and co-workers reported that for a bimetallic (NiCo) MOF, nanosheets (thickness: ≈3 nm) are much better catalysts for the oxygen evolution reaction (OER) than the bulk counterpart (Figure 2b).^[46] The authors attributed the superior performance of the nanosheets to their higher proportion of oxidized Ni, and to the greater activity of their coordinatively unsaturated Co atoms, relative to those in the counterpart. Similarly, Duan and co-workers, working with another bimetallic (NiFe) MOF as catalyst for the OER, affirmed that nanosheets of this MOF have nearly 1,000-fold the intrinsic electrical conductivity ($1 \pm 0.2 \times 10^{-3} \text{ Sm}^{-1}$) of the bulk counterpart ($1 \pm 0.5 \times 10^{-6} \text{ Sm}^{-1}$).^[47] Such enhancement is generally due to the 2D character of nanosheets, which can lead to vacancy engineering inside the material. These vacancies can act as shallow donors to increase the carrier concentration of metal octahedral units (i.e., NiFeO₆) in the MOF, thereby enhancing the conductivity. The high conductivity can facilitate charge transport during electrocatalysis, thus contributing to the higher activity of the bimetallic NiFe MOF nanosheets in the OER.

Analogous to the case of small MOF particles, 2D MOF nanofilms and nanosheets exhibit distinct flexibility profiles to their corresponding bulk counterparts. For instance, Kitagawa and co-workers showed that an oriented thin film of interdigitated 2D layers of Hofmann-type {Fe(py)₂[Pt(CN)₄]} exhibits a dynamic gate-opening response to ethanol that is not exhibited by the bulk analog (Figure 2c). The authors attributed this phenomenon to the direct correlation between the thickness of the MOF film and the diffusion length for guest molecules within that film.^[48]

In addition to endowing MOFs with two-dimensionality, miniaturization of them also opens the possibility to shape them into otherwise inaccessible morphologies such as rods, wires, tubes, or hollow spheres. For instance, Wang, Xu, and co-workers showed the synthesis of nanowires of the MOF Cu₃(2,3,6,7,10,11-hexahydroxytriphenylene)₂ catecholate (named as Cu-CAT) with dimensions of 200–250 nm diameter and 3–15 μm length.^[49] Once incorporated into an electrode, these nanowires exhibited two times higher capacitance than a similar electrode made of bulk Cu-CAT powder. According to the authors, the 1D structure of Cu-CAT nanowires significantly reduced its intrinsic resistance and charge transfer resistance at the electrode/electrolyte interface, enabling effective charge/electron transport on the interface of the nanowires array and the electrolyte. Shape-dependent behavior was also reported in NH₂-MIL-88B(Fe) nanoparticles, in which a slower but more sustainable cellular uptake was found when they were shaped into nanorods in comparison with nanooctahedra.^[50] Also, Yamahuchi and co-workers reported the synthesis of ZIF-8 nanobubbles and subsequent calcination of them into hollow carbon nanobubbles.^[51] Interestingly, for ultrafast Na⁺/K⁺ ion intercalation, the ZIF-8 nanobubbles behave like batteries, whereas the hollow carbon nanobubbles act like pseudocapacitors.

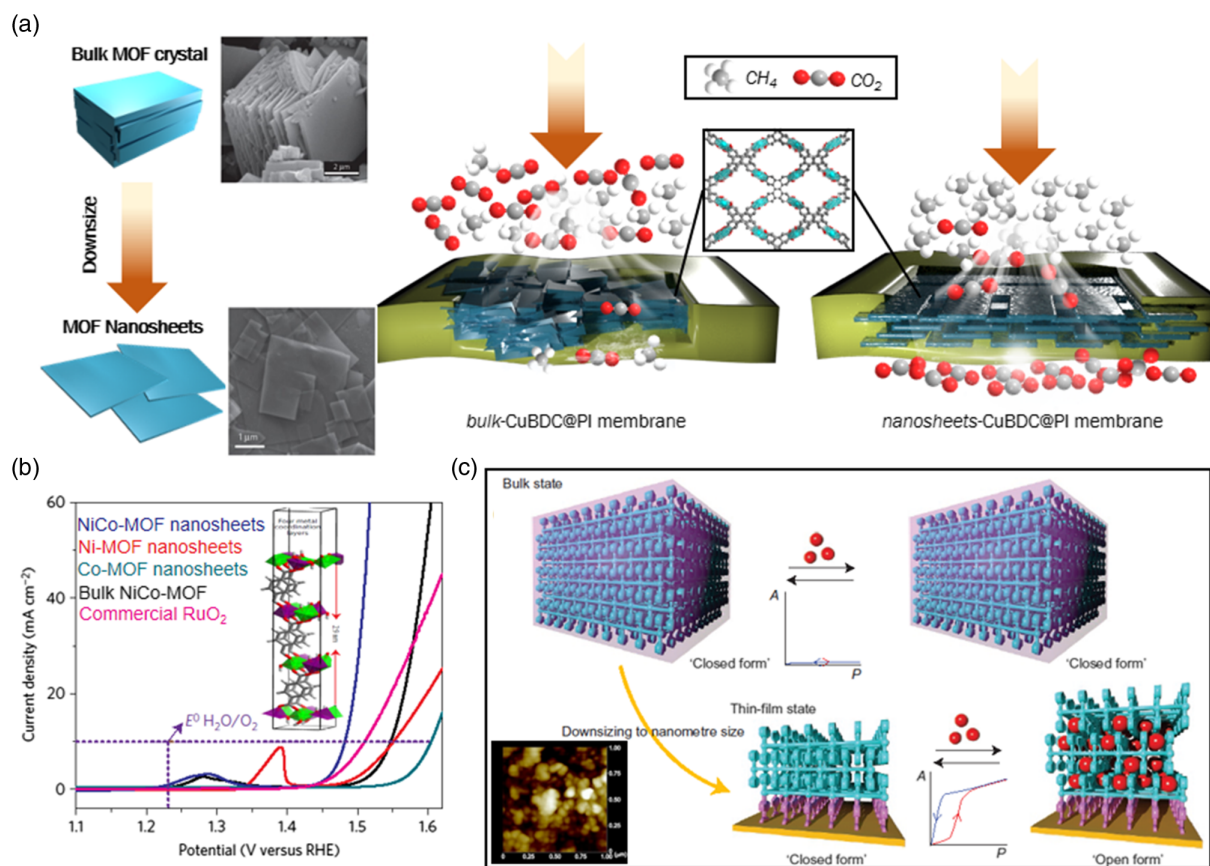


Figure 2. a) Schematic of downsizing MOFs into 2D materials (left) and their subsequent incorporation into organic polymers to generate enhanced mixed-matrix membranes for the separation of CO_2/CH_4 (right). Reproduced with permission.^[45] Copyright 2015, Nature Publishing Group. b) OER polarization curves obtained in O_2 -saturated 1 M KOH solution (scan rate; 5 mVs^{-1}) for (NiCo)-MOF nanosheets, (Ni)-MOF nanosheets, (Co)-MOF nanosheets, RuO_2 , and bulk (NiCo)-MOFs. Inset: Crystal structure indicating the theoretical thickness of the (NiCo)-MOF nanosheets. Reproduced with permission.^[46] Copyright 2016, Nature Publishing Group. c) Schematic of a crystalline coordination framework that, upon being downsized into a 2D thin film, gained the function of dynamic gate opening. Reproduced with permission.^[48] Copyright 2016, Nature Publishing Group.

4. Processability: Colloidal Dispersion, Outer Surface Functionalization, Surface Growth, and Self-Assembly

Recently, great advances have been made on the controlled synthesis of MOF particles at the submicro- and nanometer scales, allowing for excellent homogeneity in both size and shape. Such small MOFs show certain advantages over their corresponding bulk particles. First, as the size of MOF particles decreases, their propensity to Brownian motion increases. Consequently, within a suspension, small MOFs usually do not sediment, unlike larger particles, whose dynamic behavior in suspension is subject to gravity and sedimentation. Second, the large outer surface of small MOF particles can be functionalized with surfactants and/or (bio)molecules to achieve specific interactions with their environment and/or to preclude them from aggregating. Together, these advantages favor colloidal stability, which in turn translates to the ability to use readily processable MOF-based liquids in countless practical and industrial applications.

Interestingly, stable colloidal dispersions of homogeneous MOF particles can drive the construction of more sophisticated

meso- and macroscopic architectures via self-assembly, giving access to new properties such as photonic properties that arise from the periodic arrangement of such particles. For example, Maspoch and colleagues, including authors of this present review, reported that controlled evaporation of aqueous colloidal dispersions of ZIF-8 or UiO-66 particles functionalized with the surfactant cetyltrimethylammonium bromide leads to self-assembly of ordered 3D superlattices into photonic crystals (Figure 3a).^[52] Similarly, Mirkin et al. hybridized DNA to oligonucleotide-functionalized colloidal UiO-66 particles to fabricate 3D assemblies.^[53] This latter approach was also used to construct binary single crystals, comprising colloidal MOF and Au nanoparticles and 2D MOF nanorod assemblies.^[54]

Alternatively, macroscopic MOF monoliths can be fabricated by the controlled drying and gluing together of small MOF particles. For example, Fairén and co-workers developed a procedure that begins with the gelation of ultrasmall MOF (e.g., ZIF-8, HKUST-1, UiO-66, etc.) particles to prepare a family of highly dense MOF monoliths that exhibit high volumetric adsorption (Figure 3b).^[55] The products included HKUST-1 monoliths that exhibit a volumetric methane adsorption capacity of 259 cm^3

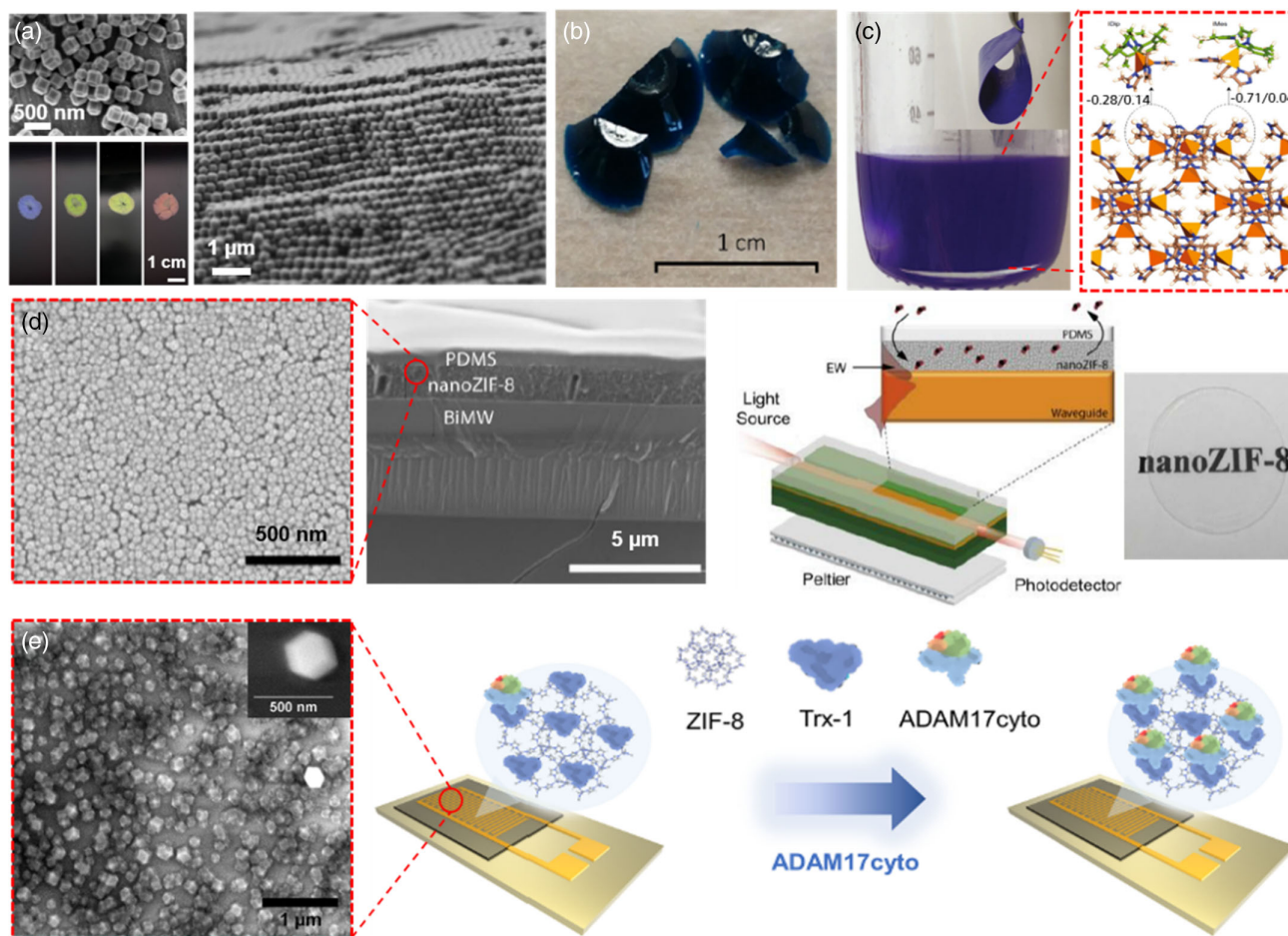


Figure 3. a) Scanning electron micrographs (top left and right) and photos (bottom left) of the self-assembly of colloidal ZIF-8 nanoparticles into an ordered 3D photonic superstructure. Reproduced with permission.^[52] Copyright 2018, Nature Publishing Group. b) Photo of an HKUST-1 monolith gel. Reproduced with permission.^[55] Copyright 2020, American Chemical Society. c) Photos of a porous liquid and a composite membrane (inset) based on N-heterocyclic carbene-functionalized ZIF-67 nanoparticles (left) and a schematic of the functionalization of ZIF-67. Reproduced with permission.^[58] Copyright 2020, Nature Publishing Group. d) Scanning electron micrographs (left) and schematic of an optical CO₂ sensor based on self-assembled, ultrasmall ZIF-8 nanoparticles (photo of the transparent film on the right). Reproduced with permission.^[57] Copyright 2018, Royal Society of Chemistry. e) Scanning electron micrograph (left) of an electrochemical biosensor based on ZIF-8 nanoparticles; and corresponding schematics of the working mechanism (middle and right). Reproduced with permission.^[62] Copyright 2021, American Chemical Society.

(STP) cm^{-3} at 65 bar, which is the highest deliverable capacity achieved by any adsorbent after successful pelletization and shaping.^[56] A similar self-assembly strategy of ultrasmall MOF particles has also been used to fabricate ZIF-8 films, which, when ZIF-8 particle size was decreased down to 32 ± 5 nm, became transparent, thus enabling integration of them into a CO₂ optical sensor (Figure 3d).^[57]

Highly stable colloidal MOF dispersions can also be obtained via postsynthetic functionalization in organic solvents. For example, Gascon and co-workers recently synthesized stable colloidal MOF dispersions in cyclohexane, cyclooctane, and mesitylene by postsynthetically modifying the outer surface of ZIF-67 particles with N-heterocyclic carbenes, such as 1,3-bis(2,4,6-trimethylphenyl)imidazole-2-ylidene and 1,3-bis(2,4,6-diisopropylphenyl)imidazole-2-ylidene.^[58] Using this chemistry, they were able to prepare porous liquids and to optimize the integration of the

functionalized ZIF-67 particles in highly loaded (47.5 wt%) mixed-matrix membranes for separation of propylene from propane (Figure 3c). In another example, Jeffrey and co-workers reported that well-dispersed MOF-74 nanocrystals in a polyimide membrane exhibited enhanced selectivity for ethylene over ethane with greater ethylene permeability. They postulated that the small crystals had a more exposed external surface area, leading to greater interaction between the polymer and the crystals and thus minimizing the number of nonselective pathways for gas transport.^[59] Likewise, Ghalei and co-workers were able to improve the selectivity of highly permeable PIM-1 mixed-matrix membranes using colloidal NH₂-functionalized UiO-66 particles to minimize nonselective microvoid formation around the particles.^[60]

In addition to their utility for preparing MOF colloids, the advances made in controlling the direct synthesis of small

MOFs facilitate surface integration of MOFs into myriad devices such as gas sensors, photonic cells, and transparent electronics. The methods developed to incorporate MOFs onto surfaces include seeding growth, layer-by-layer growth, nanolithography, and chemical vapor deposition. In these methods, MOFs are grown on surfaces using either solutions or vapors of the precursors. For example, Fischer, Wöll, and co-workers grew MOF films on surfaces by layer-by-layer growth to fabricate several MOF-based chemical sensors.^[61] Bufon, Leme, and co-workers recently used a similar approach to grow ZIF-8 on electrodes, which they used as transducers to monitor protein–protein interactions involving ADAM17cyto (Figure 3e).^[62] Alternatively, Zhang, Wang, and co-workers used a seeding-growth approach to create artificial MOF-based channels analogous to biological ion channels, which showed remarkable ion selectivity, permeability, and rectification properties.^[63] Specifically, they grew UiO-66-(COOH)₂ particles (≈43.7 nm) as embedded seeds in bullet-shaped subnanochannels to construct asymmetrically structured crystalline MOF subnanochannels. The resultant heterogeneous structure could rapidly conduct K⁺, Na⁺, and Li⁺ in the subnanometer-to-nanometer channel direction, with conductivities of up to three orders of magnitude greater than those of Ca²⁺ and Mg²⁺, equivalent to a mono/divalent ion selectivity of 103:1.

Finally, contemporary micro-/nanofabrication methods are used to manufacture MOF-based devices. For example, Ameloot and co-workers used chemical vapor deposition to create high-quality films of ZIF-8, with controlled uniform thickness.^[64] More recently, the same authors similarly grew halogenated films of ZIF-8 by chemical vapor deposition and then subjected the films to X-ray and electron beam lithography to create high-quality patterns at 50 sub-nm resolution.^[65]

5. Conclusion and Outlook

Recent advances on the miniaturization of MOFs down to the submicroscale and even the nanoscale have revealed that their properties are highly dependent on particle size and shape. At these scales, the outer surface areas of MOF crystals dictate many of their properties and regulate their interaction with surrounding media. Thus, controlling the surface area and surface composition of small MOFs is critical for tuning, reproducing, and discovering their properties. Accordingly, a pending question for researchers here is as follows: How can the area and composition of the outer surface of small MOFs be tailored? As with any other type of nanomaterial, this requires controlled synthesis of monodispersed particles at fixed sizes and shapes and surface functionalization with other molecules. Controlling these processes should also enable tuning of other parameters, such as the number of defects, which can influence the properties of MOFs at this length scale. In this context, greater efforts should be concentrated on developing methods for synthesizing monodispersed MOF particles in solution and on surfaces and for functionalizing their surface. These new chemistries should be supported through advanced techniques for molecular-scale characterization such as transmission electron microscopy,^[66] atomic force microscopy,^[67] and atom probe tomography.^[68] We are confident that such research will facilitate understanding of the behavior of

small MOFs and advance their processability; their integration into devices and films; and their use in the fabrication of macroscopic objects, liquid porous material, and composites. In this sense, we believe that the use of small MOFs as drug delivery platforms,^[69] imaging agents,^[70] catalysts,^[69] in membrane separation, and^[60] in energy,^[71] among other applications, will constantly increase in the near future.

Acknowledgements

This work was supported by the Spanish MINECO (project RTI2018-095622-B-I00), the Catalan AGAUR (project 2017 SGR 238), and the ERC, under the EU-FP7 (ERC-Co 615954). It was also funded by the CERCA Program/Generalitat de Catalunya. ICN2 was supported by the Severo Ochoa program from the Spanish MINECO (grant no. SEV-2017-0706).

Conflict of Interest

The authors declare no conflict of interest.

Keywords

colloidal metal–organic frameworks, metal–organic framework miniaturizations, MOF processabilities, size-dependent properties, 2D metal–organic frameworks

Received: July 29, 2021

Revised: September 17, 2021

Published online: October 19, 2021

- [1] H. C. Zhou, S. Kitagawa, *Chem. Soc. Rev.* **2014**, *43*, 5415.
- [2] H. C. Zhou, J. R. Long, O. M. Yaghi, *Chem. Rev.* **2012**, *112*, 673.
- [3] J. R. Long, O. M. Yaghi, *Chem. Soc. Rev.* **2009**, *38*, 1201.
- [4] M. P. Suh, H. J. Park, T. K. Prasad, D.-W. Lim, *Chem. Rev.* **2012**, *112*, 782.
- [5] Y. He, W. Zhou, G. Qian, G. B. Chen, *Chem. Soc. Rev.* **2014**, *43*, 5657.
- [6] K. Sumida, D. L. Rogow, J. A. Mason, T. M. McDonald, E. D. Bloch, Z. R. Herm, T.-H. Bae, J. R. Long, *Chem. Rev.* **2012**, *112*, 724.
- [7] D. Farrusseng, S. Aguado, C. Pinel, *Angew. Chem., Int. Ed.* **2009**, *48*, 7502.
- [8] P. Horcajada, R. Gref, T. Baati, P. K. Allan, G. Maurin, P. Couvreur, G. Ferey, R. E. Morris, C. Serre, *Chem. Rev.* **2012**, *112*, 1232.
- [9] M. F. de Lange, K. J. F. M. Verouden, T. J. H. Vlugt, J. Gascon, F. Kapteijn, *Chem. Rev.* **2015**, *115*, 12205.
- [10] L. E. Kreno, K. Leong, O. K. Farha, M. Allendorf, R. P. Van Duyne, J. T. Hupp, *Chem. Rev.* **2012**, *112*, 1105.
- [11] Y. Belmabkhout, V. Guillermin, M. Eddaoudi, *Chem. Eng. J.* **2016**, *296*, 386.
- [12] C. R. Groom, I. J. Bruno, M. P. Lightfoot, S. C. Ward, *Acta Cryst. Section B* **2016**, *72*, 171.
- [13] A. Carné, C. Carbonell, I. Imaz, D. MasPOCH, *Chem. Soc. Rev.* **2011**, *40*, 291.
- [14] M. Rubio-Martinez, C. Avci-Camur, A. W. Thornton, I. Imaz, D. MasPOCH, M. R. Hill, *Chem. Soc. Rev.* **2017**, *46*, 3453.
- [15] S. Wang, C. M. McGuirk, A. d'Aquino, J. A. Mason, C. A. Mirkin, *Adv. Mater.* **2018**, *30*, 1800202.
- [16] E. Ploetz, H. Engelke, U. Lächelt, S. Wuttke, *Adv. Funct. Mater.* **2020**, *30*, 1909062.

- [17] C. R. Marshall, S. A. Staudhammer, C. K. Brozek, *Chem. Sci.* **2019**, *10*, 9396.
- [18] X. Cai, Z. Xie, D. Li, M. Kassymova, S.-Q. Zang, H.-L. Jiang, *Coordin. Chem. Rev.* **2020**, *417*, 213366.
- [19] M. B. Majewski, H. Noh, T. Ismaglou, O. K. Farha, *J. Mater. Chem. A* **2018**, *6*, 7338.
- [20] H. Wang, B.-H. Chen, D.-J. Liu, *Adv. Mater.* **2021**, *33*, 2008023.
- [21] J. Troyano, A. Carné-Sánchez, C. Avci, I. Imaz, D. Maspoch, *Chem. Soc. Rev.* **2019**, *48*, 5534.
- [22] S. Ehrling, H. Miura, I. Senkowska, S. Kaskel, *Trends Chem.* **2021**, *3*, 291.
- [23] Y. Sakata, S. Furukawa, M. Kondo, K. Hirai, N. Horike, Y. Takashima, H. Uehara, N. Louvain, M. Meilikhov, T. Tsuruoka, S. Isoda, W. Kosaka, O. Sakata, S. Kitagawa, *Science* **2013**, *339*, 193.
- [24] D. Tanaka, A. Henke, K. Albrecht, M. Moeller, K. Nakagawa, S. Kitagawa, J. Groll, *Nat. Chem.* **2010**, *2*, 410.
- [25] T. Kundu, M. Wahiduzzaman, B. B. Shah, G. Maurin, D. Zhao, *Angew. Chem. Int. Ed.* **2019**, *58*, 8073.
- [26] M. Kriesten, J. Vargas Schmitz, J. Siegel, C. E. Smith, M. Kasperleit, M. Hartmann, *Eur. J. Inorg. Chem.* **2019**, *43*, 4700.
- [27] S. Tanaka, K. Fujita, Y. Miyake, M. Miyamoto, Y. Hasegawa, T. Makino, S. Van der Perre, J. Cousin Saint Remi, T. Van Assche, G. V. Baron, J. F. M. Denayer, *J. Phys. Chem. C* **2015**, *119*, 28430.
- [28] T. Tian, M. T. Wharmby, J. B. Parra, C. O. Ania, D. Fairen-Jimenez, *Dalton Trans.* **2016**, *45*, 6893.
- [29] S. Krause, V. Bon, I. Senkowska, D. M. Töbrens, D. Wallacher, R. S. Pillai, G. Maurin, S. Kaskel, *Nat. Commun.* **2018**, *9*, 1573.
- [30] X. Xiao, L. Zou, H. Pang, Q. Xu, *Chem. Soc. Rev.* **2020**, *49*, 301.
- [31] B. Wang, W. Liu, W. Zhang, J. Liu, *Nano Res.* **2017**, *10*, 3826.
- [32] A. Yazdi, F. Mercoçi, N. G. Bastús, I. Imaz, V. Puentes, D. Maspoch, *Catal. Sci. Tech.* **2016**, *6*, 8388.
- [33] P. Li, R. C. Klet, S.-Y. Moon, T. C. Wang, P. Deria, A. W. Peters, B. M. Klahr, H.-J. Park, S. S. Al-Juaid, J. T. Hupp, O. K. Farha, *Chem. Commun.* **2015**, *51*, 10925.
- [34] T. Kiyonaga, M. Higuchi, T. Kajiwara, Y. Takashima, J. Duan, K. Nagashima, S. Kitagawa, *Chem. Commun.* **2015**, *51*, 2728.
- [35] O. M. Linder-Patton, T. J. de Prinse, S. Furukawa, S. G. Bell, K. Sumida, C. J. Doonan, C. J. Sumbly, *CrystEngComm.* **2018**, *20*, 4926.
- [36] M. Zhong, L. Kong, K. Zhao, Y.-H. Zhang, N. Li, X.-H. Bu, *Adv. Sci.* **2021**, *8*, 2001980.
- [37] P. Xiao, F. Bu, R. Zhao, M. F. Aly Aboud, I. Shakir, Y. Xu, *ACS Nano* **2018**, *12*, 3947.
- [38] J. Castells-Gil, S. Ould-Chikh, A. Ramírez, R. Ahmad, G. Prieto, A. R. Gómez, L. Garzón-Tovar, S. Telalovic, L. Liu, A. Genovese, N. M. Padial, A. Aguilar-Tapia, P. Bordet, L. Cavallo, C. Martí-Gastaldo, J. Gascon, *Chem Catal.* **2021**, *1*, 1.
- [39] J. Liu, X. Song, T. Zhang, S. Liu, H. Wen, L. Chen, *Angew. Chem. Int. Ed.* **2021**, *60*, 5612.
- [40] H. Zhu, D. Liu, *J. Mater. Chem. A* **2019**, *7*, 21004.
- [41] K. W. Nam, S. S. Park, R. dos Reis, V. P. Dravid, H. Kim, C. A. Mirkin, J. F. Stoddart, *Nat. Commun.* **2019**, *10*, 4948.
- [42] J. López-Cabrelles, S. Mañas-Valero, I. J. Vitorica-Yrezábal, P. J. Bereciartua, J. A. Rodríguez-Velamazán, J. C. Waerenborgh, B. J. C. Vieira, D. Davidovikj, P. G. Steeneken, H. S. J. van der Zant, G. Mínguez Espallargas, E. Coronado, *Nat. Chem.* **2018**, *10*, 1001.
- [43] Y. Peng, Y. Li, Y. Ban, H. Jin, W. Jiao, X. Liu, W. Yang, *Science* **2014**, *346*, 1356.
- [44] J. H. Dou, M. Q. Arguilla, Y. Luo, J. Li, W. Zhang, L. Sun, J. L. Mancuso, L. Yang, T. Chen, L. R. Parent, G. Skorupsk, N. J. Libretto, C. Sun, M. C. Yang, P. V. Dip, E. J. Brignole, J. T. Miller, J. Kong, C. H. Hendon, J. Sun, M. Dincă, *Nat. Mater.* **2021**, *20*, 222.
- [45] T. Rodenas, I. Luz, G. Prieto, B. Seoane, H. Miro, A. Corma, F. Kapteijn, F. X. Llabrés i Xamena, J. Gascon, *Nat. Mater.* **2015**, *14*, 48.
- [46] S. Zhao, Y. Wang, J. Dong, C.-T. He, H. Yin, P. An, K. Zhao, X. Zhang, C. Gao, L. Zhang, J. Lv, J. Wang, J. Zhang, A. M. Khattak, N. A. Khan, Z. Wei, J. Zhang, S. Liu, H. Zhao, Z. Tang, *Nat. Energy* **2016**, *1*, 16184.
- [47] J. Duan, S. Chen, C. Zhao, *Nat. Commun.* **2017**, *8*, 15341.
- [48] S. Sakaida, K. Otsubo, O. Sakata, C. Song, A. Fujiwara, M. Takata, H. Kitagawa, *Nat. Chem.* **2016**, *8*, 377.
- [49] W.-H. Li, K. Ding, H.-R. Tian, M.-S. Yao, B. Nath, W.-H. Deng, Y. Wang, G. Xu, *Adv. Funct. Mater.* **2017**, *27*, 1702067.
- [50] S.-N. Kima, C. G. Park, C. H. Min, S. H. Lee, Y. Y. Lee, N. K. Lee, Y. Bin Choy, *J. Ind. Eng. Chem.* **2021** <https://doi.org/10.1016/j.jiec.2021.08.042>.
- [51] W. Zhang, X. Jiang, Y. Zhao, A. Carné-Sánchez, V. Malgras, J. Kim, J. H. Kim, S. Wang, J. Liu, J.-S. Jiang, Y. Yamauchi, M. Hu, *Chem. Sci.* **2017**, *8*, 3538.
- [52] C. Avci, I. Imaz, A. Carné-Sánchez, J. A. Pariente, N. Tasios, J. Pérez-Carvajal, M. I. Alonso, A. Blanco, M. Dijkstra, C. López, D. Maspoch, *Nature Chem.* **2018**, *10*, 78.
- [53] W. Morris, W. E. Briley, E. Auyeung, M. D. Cabezas, C. A. Mirkin, *J. Am. Chem. Soc.* **2014**, *136*, 7261.
- [54] S. Wang, S. S. Park, C. T. Buru, H. Lin, P.-C. Chen, E. W. Roth, O. K. Farha, C. A. Mirkin, *Nat. Commun.* **2020**, *11*, 2495.
- [55] B. M. Connolly, D. G. Madden, A. E. H. Wheatley, D. Fairen-Jimenez, *J. Am. Chem. Soc.* **2020**, *142*, 8541.
- [56] T. Tian, Z. Zeng, D. Vulpe, M. E. Casco, G. Divitini, P. A. Midgley, J. Silvestre-Albero, J.-C. Tan, P. Z. Moghadam, D. Fairen-Jimenez, *Nat. Mater.* **2018**, *17*, 174.
- [57] B. Chocarro-Ruiz, J. Pérez-Carvajal, C. Avci, O. Calvo-Lozano, M. I. Alonso, D. Maspoch, L. M. Lechuga, *J. Mater. Chem. A* **2018**, *6*, 13171.
- [58] A. Knebel, A. Bavykina, S. J. Datta, L. Sundermann, L. Garzon-Tovar, Y. Lebedev, S. Durini, R. Ahmad, S. M. Kozlov, G. Shterk, M. Karunakaran, I. D. Carja, D. Simic, I. Weilert, M. Klüppel, U. Giese, L. Cavallo, M. Rueping, M. Eddaoudi, J. Caro, J. Gascon, *Nat. Mater.* **2020**, *19*, 1346.
- [59] J. E. Bachman, Z. P. Smith, T. Li, T. Xu, J. R. Long, *Nat. Mater.* **2016**, *15*, 845.
- [60] B. Ghalei, K. Sakurai, Y. Kinoshita, K. Wakimoto, Ali P. Isfahani, Q. Song, K. Doitomi, S. Furukawa, H. Hirao, H. Kusuda, S. Kitagawa, E. Sivaniah, *Nat. Energy* **2017**, *2*, 17086.
- [61] O. Shekhah, J. Liu, R. A. Fischer, C. Wöll, *Chem. Soc. Rev.* **2011**, *40*, 1081.
- [62] L. D. Trino, L. G. S. Albano, D. C. Granato, A. G. Santana, D. H. S. de Camargo, C. C. Correa, C. C. Bof Bufon, A. F. Paes Leme, *Chem. Mater.* **2021**, *33*, 1293.
- [63] J. Lu, H. Zhang, J. Hou, X. Li, X. Hu, Y. Hu, C. D. Easton, Q. Li, C. Sun, A. W. Thornton, M. R. Hill, X. Zhang, G. Jiang, J. Z. Liu, A. J. Hill, B. D. Freeman, L. Jiang, H. Wang, *Nat. Mater.* **2020**, *19*, 767.
- [64] I. Stassen, M. Styles, G. Greci, Hans V. Gorp, W. Vanderlinden, Steven D. Feyter, P. Falcaro, D. D. Vos, P. Vereecken, R. Ameloot, *Nat. Mater.* **2016**, *15*, 304.
- [65] M. Tu, B. Xia, D. E. Kravchenko, M. L. Tietze, A. J. Cruz, I. Stassen, T. Hauffman, J. Teyssandier, S. De Feyter, Z. Wang, R. A. Fischer, B. Marmiroli, H. Amenitsch, A. Torvisco, M. D. J. Velásquez-Hernández, P. Falcaro, R. Ameloot, *Nat. Mater.* **2021**, *20*, 93.
- [66] X. Gong, K. Gnanasekaran, Z. Chen, L. Robison, M. C. Wasson, K. C. Bentz, S. M. Cohen, O. K. Farha, N. C. Gianneschi, *J. Am. Chem. Soc.* **2020**, *142*, 17224.
- [67] C.-H. Shu, Y. He, R.-X. Zhang, J.-L. Chen, A. Wang, P.-N. Liu, *J. Am. Chem. Soc.* **2020**, *142*, 16579.

- [68] Z. Ji, T. Li, O. M. Yaghi, *Science* **2020**, 369, 674.
[69] X. Cai, Z. Xie, D. Li, M. Kassymov, S.-Q. Zang, H.-L. Jiang, *Coord. Chem. Rev* **2020**, 417, 213366.
[70] F. D. Duman, R. Forgan, *J. Mater. Chem. B* **2021**, 9, 3423.
[71] S. Kuyuldar, D. T. Genna, C. Burda, *J. Mater. Chem. A* **2019**, 7, 21545.